AWARD NUMBER: W81XWH-10-1-0393

TITLE: Commissioning and Characterization of a Dedicated High-Resolution Breast PET Camera

PRINCIPAL INVESTIGATOR: Arne Vandenbroucke, Ph.D.

CONTRACTING ORGANIZATION: Stanford University
Stanford, CA 94305

REPORT DATE: February 2014

TYPE OF REPORT: Annual Summary

PREPARED FOR: U.S. Army Medical Research and Materiel Command
Fort Detrick, Maryland 21702-5012

REPORT DOCUMENTATION PAGE

Form Approved
OMB No. 0704-0188

1. REPORT DATE *(DD-MM-YYYY)*	2. REPORT TYPE	3. DATES COVERED *(From - To)*
Feb 2014	Annual Summary	15 Jun 2010 – 14 Nov 2013

4. TITLE AND SUBTITLE
Commissioning and Characterization of a Dedicated High-Resolution Breast PET Camera

5a. CONTRACT NUMBER

5b. GRANT NUMBER
W81XWH-10-1-0393

5c. PROGRAM ELEMENT NUMBER

6. AUTHOR(S)
Arne Vandenbroucke arnevdb@stanford.edu

5d. PROJECT NUMBER

5e. TASK NUMBER

5f. WORK UNIT NUMBER

7. PERFORMING ORGANIZATION NAME(S) AND ADDRESS(ES)
Stanford University , Stanford CA 94305-2004

8. PERFORMING ORGANIZATION REPORT NUMBER

9. SPONSORING / MONITORING AGENCY NAME(S) AND ADDRESS(ES)
U.S. Army Medical Research and Materiel Command
Fort Detrick, Maryland 21702-5012

10. SPONSOR/MONITOR'S ACRONYM(S)

11. SPONSOR/MONITOR'S REPORT NUMBER(S)

12. DISTRIBUTION / AVAILABILITY STATEMENT
Approved for public release; distribution unlimited

13. SUPPLEMENTARY NOTES

14. ABSTRACT

The high-resolution breast camera under development for this project consists of many detector modules formed by coupling pairs of high resolution scintillation crystal arrays to position sensitive avalanche photodiodes (PSAPDs). These LYSO crystal arrays contain 64 1mm^3 crystal elements. The modules are organized in cartridges built out of 8 layers of 16 modules each. During this funding cycle the two cartridges constructed in the previous cycle were further characterized in terms of uniformity and isotropy of the spatial resolution in 3D. Using multiple radioactive sources we also confirmed a linear response. Furthermore, improved calibration and thermal regulation yielded improved images compared to the ones presented in the FY03 report.
Reportable outcomes include 3 conference records, 1 book chapter, and 3 submissions to peer reviewed journals, these are still under review.

15. SUBJECT TERMS
Breast Cancer imaging, high resolution, PET camera

16. SECURITY CLASSIFICATION OF:			17. LIMITATION OF ABSTRACT	18. NUMBER OF PAGES	19a. NAME OF RESPONSIBLE PERSON
a. REPORT	b. ABSTRACT	c. THIS PAGE	UU	14	USAMRMC
U	U	U			19b. TELEPHONE NUMBER *(include area code)*

Contents

1 Introduction

The DOD funded project titled 'Commissioning and Characterization of a Dedicated High-Resolution Breast PET Camera' aims at enhancing the role of PET in breast cancer management by constructing a high resolution PET camera. PET is an imaging modality whereby lesions are visualized based on biochemical activity, rather than lesions' morphology, which is visualized by other imaging modalities such as mammography, MRI, and ultrasound. We will test this high-resolution PET system in the following indications: (1) resolving inconclusive screening mammograms which often show up for patients with dense breasts, (2) enhance staging accuracy, and (3) monitor the response to neo-adjuvant therapy. Dedicated high-resolution cameras can detect smaller lesions and thus enhance the precision of the images. Because of their high sensitivity these cameras can also reduce the injected patient dose. We aim to achieve 1 mm^3 resolution using a unique detector design that is able to measure annihilation radiation coming from the PET tracer in 3 dimensions, using many $1 \times 1 \times 1$ mm^3 scintillation crystals.

This is an *annual report* that covers progress during the No-Cost Extension period that was granted for this proposal (NCX). The NCX was requested needed in order to perform 3-D resolution studies and further characterize the constructed prototype of the breast camera in more detail.

2 Body: Research accomplishments as outlined in SOW

2-SA1 Building a block setup: months 1-6

Goal of the first task in this project was to test camera detection concepts, obtain experience working with many channels and perform image reconstruction. We used dual modules that each contain 2 position sensitive avalanche photodiodes (PSAPDs) coupled to 8×8 array of $1 \times 1 \times 1$ mm^3 LYSO crystals. The two PSAPDs are mounted on a thin flexible circuit and are multiplexed as described in [1]. As mentioned in previous years' annual report we completed this task in FY02 [2], due to significant delays caused by a required redesign of the setup due to substantial electromagnetic interference.

2-SA2 Acceptance test of the LSO-PSAPD modules: months 7-15

As reported in FY01 annual report the acceptance testing was delayed due to HV problems. Delivery of 'hot' modules started in the 5th month of FY02 (November 2011). As of January 2014 over 1,500 modules were received of the the total 2400. These modules all went through our acceptance test with an acceptance rate of about 85 %. During the period covered in this report significant time was spent to increase the speed of the module testing setup. We implemented ethernet based readout that has a higher throughput rate compared to the USB2 communication protocol. A test stand was built that allows up to 8 modules to be tested simultaneously. A photograph of the test-stand is shown in Figure 1. A holding structure for the 8 modules under test can be appreciated form the figure, as well as subsequent readout and communication electronics. Software analysis needed to be written that was able to process data from all these 8 modules. With this setup we can test about 16-24 modules per day, which is almost as fast as anticipated (4 / hour), despite the requirement of obtaining calibration data at multiple bias voltages to ensure we are selecting the correct bias voltage. Reference [3] mentions the effects of bias voltage on the PSAPD performance.

The project delay that occured during the first funding year resulted in a delayed module production. RMD Inc., the manufacturer of the dual modules was unable to speed up production

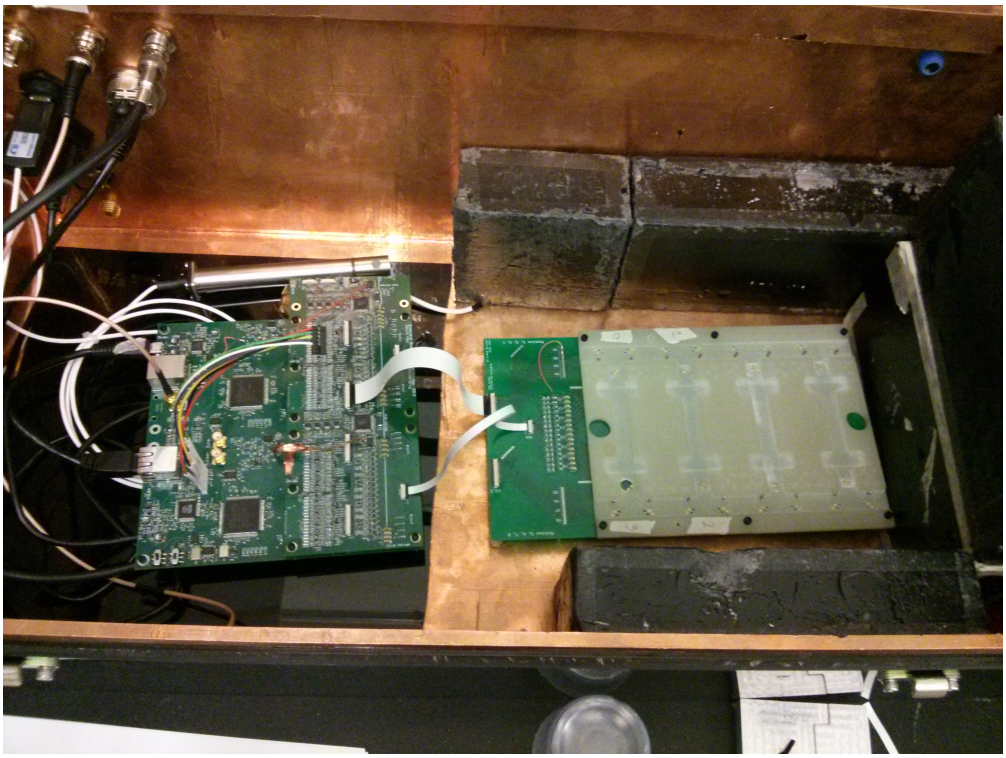

Figure 1: Photograph of the new module test setup. On the right a holding fixture with room for 8 modules can be seen. This fixture is connected to a data-acquisition board that uses the ethernet protocol for communication with the host PC

and hence the delayed start propagated through the entire project. Currently modules are produced at an average rate of 13.5 per week. Assembly of these modules is a tedious effort.

Since this project is a sequential effort, the aforementioned delay resulted in delay towards all specific aims. Nonetheless we were able to build a significant portion of the camera and study its functionality.

2-SA3 Camera Construction: months 16-26

2-SA3-A Assembly of one panel and testing: months 16-22

As mentioned in the FY03 report, we managed to fully construct 2 cartridges and operate these in coincidence in FY03. Each cartridge consists of 8 layers of 16 modules arranged side-by-side. Each cartridge thus has 128 modules, or 256 PSAPDs. We operated the system with all final electronics and readout paths as intended in the final camera.

The electronics developed and optimized includes (1) the high voltage (HV) board, which distributes HV to each individual module, (2) the signal conditioning board with bias resistors and attenuation circuitry, (3) the RENA board, responsible for charge amplification and digitization and (4) the data acquisition board (DAQ), needed for communication with the computer. All circuit boards are labeled in the photograph on the right panel of Figure 2. The left panel of the figure shows a picture of the two cartridges, along with the coordinate system used in this report.

In order to measure the intrinsic spatial resolution of the system with all finalized electronics in place, we measured the point-spread function (PSF) by stepping a radioactive ^{22}Na source across

the front face of a crystal array and measure the response of opposing crystal pairs. Doing so we obtained an intrinsic spatial resolution of 0.84 ± 0.02 mm, which is below the design goal of 1 mm (see FY03 report).

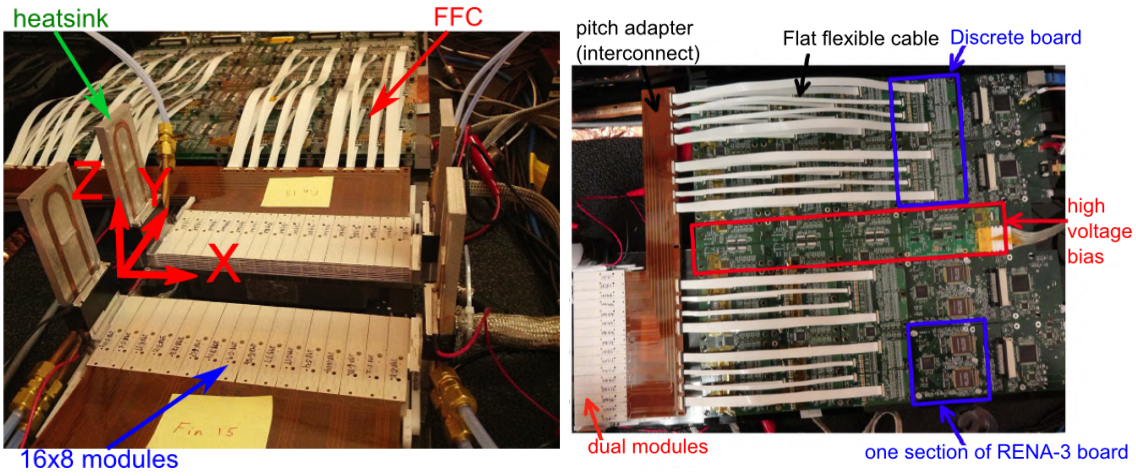

Figure 2: The **left** panel shows a photograph of the completed part of the camera. Two panels with each 8 layers of 16 dual modules can be seen. A water cooled heatsink is visible as well. Flat Flexible Cables (FFC) that lead to the back-end electronics are also indicated in the figure. The coordinate system used in this report is indicated as well. The picture on the **right** shows a top view of one panel. Various system components are indicated in the figure: (1) High voltage board, (2) signal conditioning board, (3) RENA board. The data acquisition board (4) is on the rightmost side of the figure. The picture also shows dual modules and FFC interconnects

2-SA3-B Finish construction of the Camera: months 23-26

Due to the delays mentioned in section 2-SA2 we were not able to finish the construction of the camera as a whole. However we did build a significant fraction of the camera. Due to the modular nature of our design, it is expected that adding subsequent cartridges would be straightforward.

In addition to finalizing cartridge assembly and electronics, we also wrote software that programs and reads out the constructed cartridges, and assembly procedures were finalized.

Due to the strong relationship between performance and temperature of a PSAPD [3] (see figure 3, right), it is mandatory to implement thermal regulation in the design. We use aluminum *fins* which the modules are mounted to using a miniature screw. These fins conduct the produced heat (about 3 mW per fin) to the edge of the detector panels. A thermoelectric (Peltier) element is located at both edges. The hot side of the Peltier element is cooled by a water cooled heat-sink. Each *fin* includes a thermistor for temperature readout so a feedback loop can be established.

During this funding cycle we studied the repeatability of the cooling and the bias voltage lines. From a system perspective it is important that the same operating conditions are achieved after turning the system off and back on. In order to study this repeatability, we turned the system on on 3 different days and we measured the gain. Due to its strong dependence on both bias voltage and temperature (see above), gain is a good indication of system stability. The center panel of figure 3 shows the average 511 keV photopeak shift from the mean postion. We see that differences of maximum ± 5 keV or $\pm 1\%$ can be seen. This indicates that the system can reliably be brought to the same operating conditions, even after power-cycling. The graph indicates that

we have developed a reliable thermal regulation system and that we have the bias voltage supply lines under control.

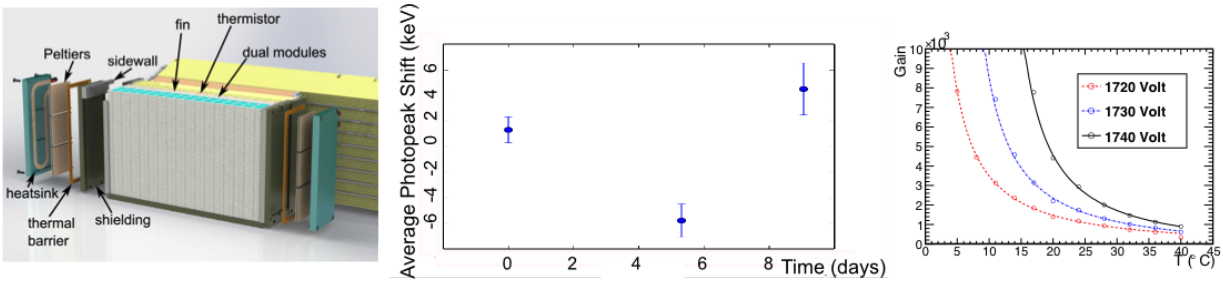

Figure 3: Left Implementation of the cooling in our design. Side-walls, shielding, thermoelectric elements and liquid heat sink are shown in the figure. **Middle:** Average photopeak position shift from the mean for data taken over a 10-day period, after switching the system on and off. Only a small deviation of roughly ±5 keV is observed. **Right:** gain as a function of temperature at different bias voltages.

2-SA4 Commissioning and Characterization of the Camera: months 27-32

Due to the aforementioned delays we performed commissioning and characterization of the camera with part of the camera only. Nonetheless this study yields important insights in camera performance and characterization.

The FY03 report presented data from 444 of 512 (= 87%) crystal arrays/PSAPDs, and showed a system-wide energy resolution of $10.62 \pm 0.04\%$ FWHM at 511 keV. We also showed that the energy resolution was uniform across all modules. The same report mentioned at timing resolution of 12.2 ± 0.2 ns.

One important aspect of the system is its linearity. In particular, if multiple photon interactions are to be used in the reconstructed images. We investigated system linearity by using ^{57}Co (122 keV), ^{22}Na (511 keV), ^{133}Ba (303 and 358 keV) and ^{137}Cs (662 keV). The top of figure 4 shows the linearity of the response. A straight line fits the data well. The bottom panel in the same figure shows the energy resolution at each of these energies. The resolution follows a $p_0 + \frac{p_1}{\sqrt{E}}$ distribution as expected from first principles (with p_0 and p_1 fit parameters). Since the energy resolution follows the theoretical distribution we show that we have noise under control in our system

Spatial resolution (point spread function (PSF)) was measured in the previous funding cycle by stepping a 0.25 μm point source in 100 μm steps across the face of the two opposing cartridges, and counting the coincidence events in opposing crystal pairs (see FY03 report). Doing so, the PSF is obtained, which was measured to be 0.84 ± 0.02 mm on average, again using all electronics and interconnects to be used in the final system. During the last funding cycle we investigated uniformity and isotropy of the spatial resolution. To do so we positioned a ^{22}Na source at 7 distinct locations in the center of the field of view, each location being 20 mm apart. We reconstructed images using 5 MLEM iterations and determined resolution in x, y and z respectively by estimating the FWHM of the projection of the point source in respective directions. Although iterative reconstruction methods are known to potentially artificially boost spatial resolution, we used iterative methods because of the difficulties associated with 3-D filtered back projection, in particular when not all angles are sampled as is the case in our system that has limited angle tomography.We tried to mitigate the overestimation of the spatial resolution by limiting the reconstruction to 5 iterations.

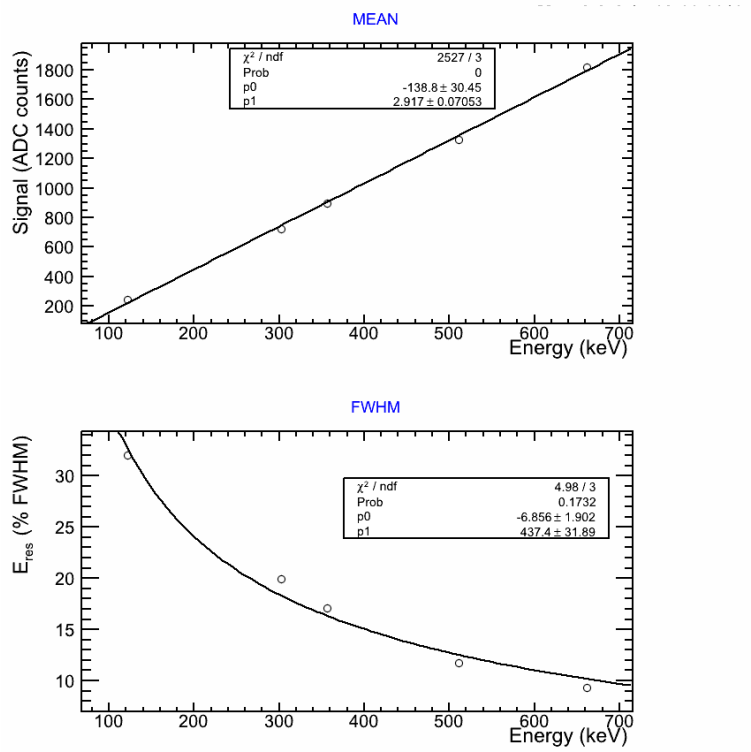

Figure 4: Top: ADC response for different isotopes: ^{57}Co (122 keV), ^{22}Na (511 keV), ^{133}Ba (303 and 358 keV) and ^{137}Cs (662 keV). A straight line was fit to the data points. **Bottom:** Energy resolution at these energies. A $\frac{1}{\sqrt{E}}$ function was fit to the data.

Fig 5 shows the resolution in X, Y and Z for all 7 positions (see figure 2 for axis orientation). We see that the system response is both isotropic and uniform in the X and Z direction. The Y resolution is slightly worse than the X and Z resolutions, however this anisotropy is much better than in a commercially available dedicated breast PET system [5]. The resolution in Y also portrays a non-uniformity. The resolution is degraded near the edges of the field-of-view. In particular for position 7 the resolution is degraded. In that region of the camera we had to disconnect several modules due to HV problems. In order to mitigate these HV problems, and in order to retain as much of the system as possible, even in the case of breakdown of some of the modules, we redesigned some of the system by placing bias resistors on the pitch adapter, i.e. closer to the modules. As such, if one module breaks down, all other modules in the same segment should still be operational. We also want to stress that this data is likely to improve when more cartridges will be added to the setup.

We also investigated methods to improve the reconstruction of the micro-Derenzo phantom that we initiated in the previous funding cycle. The phantom can be seen in the left panel of figure 6. For reference, the reconstructed phantom in FY03 is also portrayed in the middle panel of the figure. Improvements in alignment, calibration software, cooling, and normalization have resulted in a much improved reconstructed image, seen on the right of the figure. The 1.6 mm spheres appear much sharper. Although we only used a small subset of the final system (i.e. small number of counts) and non-optimal normalization code, the 1.2 mm spheres are distinctly visible. We used 60 iterations and post-corrected the image with subtraction of randoms, which were determined

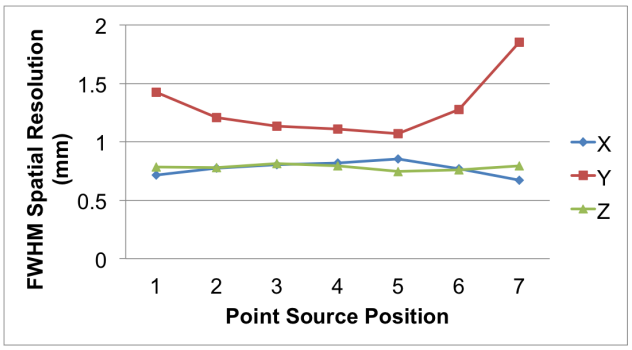

Figure 5: Reconstructed FWHM resolution at 7 different positions in the center of the field-of-view (each being 20 mm apart). FWHM was determined from a projection of the 3-D reconstructed data using MLEM and 5 iterations.

using the delayed coincidence method. WE believe that further reconstruction improvements, in particular regarding the normalization will further enhance the image quality.

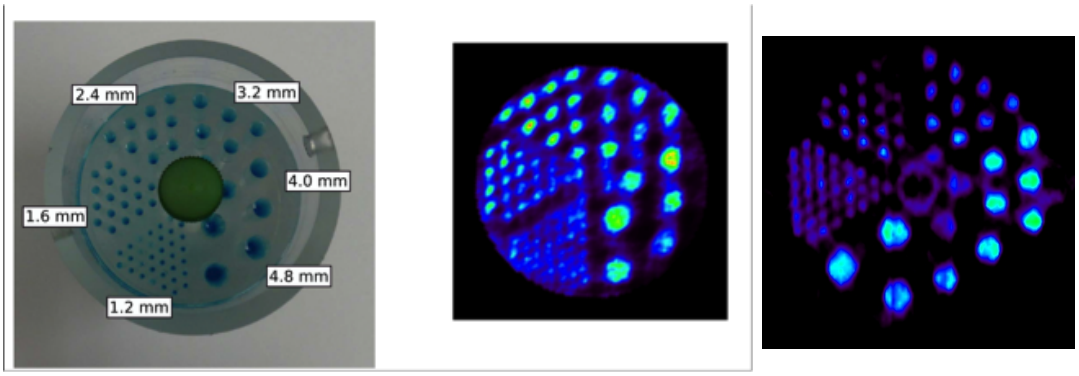

Figure 6: Left: Photograph of the micro derenzo phantom. Cylinder diameters are indicated in the figure. **Middle:** Reconstructed image as portrayed in the FY03 report. **Right:** Reconstructed image of the derenzo phantom using improved methodology described in this report. Note that the image of the phantom on the right is rotated clockwise by 60°, compared to the picture on the left.

2-SA5 Prepare patient studies: months 33-36

Due to the aforementioned delays, patient studies could not be prepared. However, we met several times with Dr. Ikeda, head of the Stanford Breast Imaging Center, and with Dr. Wapnir, Chief of Breast Surgery at Stanford to re-iterate the first studies with this camera. Consensus was to aim at two pilot studies. For Pilot Study I, 10 patient will be recruited that are undergoing a regular staging PET/CT. We will image with the novel two-panel system after the standard PET/CT scan, in order not to interfere with the standard practice of care. In addition, we won't need to administer FDG for the sole purpose of the study: we will image with the remainder of the activity. This study will allow us to compare performance of our camera with standard PET/CT imaging devices, albeit at an effective lower dose. We will evaluate and compare lesion size, contrast and standard uptake value (SUV).

Pilot Study II will validate the utility of 1 mm^3 resolution breast-dedicated PET in 10 women with newly diagnosed breast cancer who harbor other lesions in either breast that will be biopsied.

Preferably these patients will have had an MRI scan so we can compare outcome of our system with the results of an MRI system and pathology.

3 Key Research Accomplishments

- Built an improved setup for module testing that enables a higher throughput.
- Determined the repeatability of the operating conditions by analyzing PSAPD gains on different dates. Less than 1% variation in gain was determined
- Verified linearity of the constructed prototype using 4 different isotopes. Response was linear up to 662 keV
- Studied isotropy and uniformity in 3 dimensions. Spatial resolution is uniform and isotropic in X and Z, acceptable non-uniformity and non-isotropy was measured in Y.
- Improved calibration, cooling and image reconstruction methods lead to a much improved image of the reconstructed micro-derenzo phantom.
- About 55 % of the modules to be used in the final system are tested and 80 % of those are accepted.

4 Reportable Outcomes

4.1 Publications

- Three papers are currently under review:

  1. A. Vandenbroucke and C.S. Levin *Identifying and sorting crystal pixel locations in position sensitive detectors using pictorial structures*, submitted to Medical Physics
  2. J. Zhai, A. Vandenbroucke, C.S. Levin *Thermal Regulation for APDs in a 1 mm^3 Resolution Clinical PET Camera: Design, Simulation and Experimental Verification*, submitted to Physics in Medicine and Biology
  3. P.D. Reynolds, F.W.Y. Lau, A. Vandenbroucke, D. Innes, U. Yoruk, D. Freese and C.S. Levin *Performance Characterization of Two Sections of a 1 mm3 Resolution Clinical PET System*, submitted to Physics in Medicine and Biology

4.2 Conference Records

1. A. Vandenbroucke, P. D. Reynolds, F. W. Lau, D. Innes, A. Mihlin, D. L. Freese, D. F. Hsu, C. S. Levin: *First Measurements of a 512 PSAPD Prototype of a Sub-MM Resolution Clinical PET Camera*, *IEEE Nuc. Sci. Conf. Rec* **2013**, in print

2. D. L. Freese, A. Vandenbroucke, D. Innes, F. W. Y. Lau, D. Hsu, P. D. Reynolds, C. S. Levin: *Current and Temperature monitoring and thermal regulation performance of a clinical PET system consisting of many APDsIEEE Nuc. Sci. Conf. Rec* **2013**, in print

3. S. Cui, A. Vandenbroucke, M. Bieniosek, and C.S. Levin: *General spatial distortion correction method for solid-state position sensitive detectors in PET IEEE Nuc. Sci. Conf. Rec* **2013**, in print

4.3 Book Chapter

1. A. Vandenbroucke, C.S. Levin *Engineering the next generation PET detectors*, *Engineering in Translational Medicine*, edited by W. Cai, Springer, 2014

5 Conclusions

Significant progress towards completion of the 1 mm^3 resolution breast specific PET camera was made during the NCE extention into the fourth funding year. We have received about 55 % of the modules and about 80 % of these passed our functionality criteria. We managed to construct 2 cartridges, with 256 dual modules each. We connected these to the readout electronics that we will use in the final system.

The module test-stand, used to determine module functionality and ideal bias voltage was upgraded. The re-engineered test stand can now handle 8 dual LYSO-PSAPD modules, compared to only one for the previous setup.

We characterized the two cartridges developed in the previous funding cycle. These cartidges include the finalized signal conditioning [4] and readout electronics, as well as the high voltage biasing circuitry. A global energy resolutions of 10.62 ± 0.04 % FWHM was obtained for the entire system. A global coincidence time resolution of 12.2 ± 0.2 ns FWHM was measured.

Linearity was determined using 4 different isotopes and analyzing the photopeak position of these. We indeed measure linear response for these sources, and also measured an expected $\frac{1}{\sqrt{E}}$ dependence of the energy resolution, showing that no significant noise sources are present, and that the energy resolution is determined by Poisson statistics only.

We measured an intrinsic spatial resolution of 0.84 ± 0.02 mm, which is below the design goal of 1 mm. This high spatial resolution is partly due to a low average misidentification rate of < 1 %. Furthermore we investigated isotropy and uniformity. We measured an average resolution of 0.775 ± 0.057 cm in X, 0.782 ± 0.022 cm in Z, and 1.296 ± 0.272 cm in Y. These comparison of the average resolution shows an isotropic resolution in X and Z, with a slight non-isotropy in Y. The standard deviations show a uniformity in X and Z, and a small non-uniformity in Y. These results were obtained using a ^{22}Na point source.

During this last funding cycle we also showed an improved reconstructed image quality of the micro-Derenzo phantom. We improved thermal regulation, normalization and calibration methods which resulted in the distinguished appearance of the smallest spheres in the micro Derenzo phantom, and a significant visual imporvement of the reconstructed image.

Despite significant project delay, the reported results show that we made good progress towards construction of the breast dedicated PET camera described in the project. We have overcome significant technical problems. We plan to utilize the 1mm^3 resolution PET camera to assist in breast cancer management by resolving inconclusive mammograms, performing local staging and analyzing response to therapy.

References

[1] Lau F W Y, Vandenbroucke A, Reynolds P D, Olcott P D et al. Analog signal multiplexing for PSAPD-based PET detectors: simulation and experimental validation *Phys. Med. Biol.* **55**, 7149, 2010

[2] A. Vandenbroucke, F.W.Y. Lau, P.D. Reynolds, C.S. Levin Measuring 511 keV Photon Interaction Locations in Three Dimensional Position Sensitive Scintillation Detectors *Nuc. Sci. Conf. Rec* **2011**, p 3635-3638, 2011

[3] A. Vandenbroucke, T.J. McLaughlin, C.S. Levin Performance evaluation of a large area position sensitive avalanche photodiode coupled to an LSO crystal array as a function of temperature and bias voltage *J. Inst* **7**, P08001, 2012

[4] F.W.Y Lau, A. Vandenbroucke, P.D. Reynolds, H. Ho, D. Innes, C.S. Levin Signal Conditioning Technique for Position Sensitive Photodetectors to Manipulate Pixelated Crystal Identification Capabilities *IEEE Trans. Nucl. Sci*, **59**, 1815-1822, 2012

[5] W. Luo, E. Anashkin, C.G. Matthews Performance Evaluation of a PEM Scanner Using the NEMA NU 4-2008 Small Animal PET Standards, *IEEE Trans. Nucl. Sci*, **57**, 94-103, 2010